Available online at www.sciencedirect.com
SCIENCE DIRECT®
Nuclear Physics A 767 (2006) 155–170
NUCLEAR PHYSICS A

Short-range correlations in two-nucleon knockout reactions

C.A. Bertulani

Department of Physics, University of Arizona, Tucson, AZ 85721, USA

Received 11 July 2005; received in revised form 24 November 2005; accepted 20 December 2005

Available online 11 January 2006

Abstract

A theory of short-range correlations in two-nucleon removal due to elastic breakup (diffraction dissociation) on a light target is developed. Fingerprints of these correlations will appear in momentum distributions of back-to-back emission of the nucleon pair. Expressions for the momentum distributions are derived and calculations for reactions involving stable and unstable nuclear species are performed. The signature of short-range correlations in other reaction processes is also studied.

PACS: 21.10.Jx; 24.50.+g; 25.60.-t; 27.20.+n

Keywords: Knockout reactions; Short-range correlations; Momentum distributions

1. Introduction

A primary goal of nucleus–nucleus scattering has been to learn about nuclear structure. This has become even more critical in recent years, when many groups became very active in the investigation of the physics of nuclei far from the stability, mainly using nucleus–nucleus scattering processes at intermediate energies ($E_{\rm lab} \simeq 100$ MeV/nucleon). The theoretical complexity of such collisions has given rise to the use of a number of different approximations. The adequate theoretical tool for this purpose is Glauber's multiple-scattering theory [1]. It has long been known both for its simplicity and amazing predictive power. One can find copious examples in the literature where the Glauber theory allows for a simple physical interpretation of experimental results as well as their quantitative analysis [2–4]. In fact, fragmentation reactions

E-mail address: bertulani@physics.arizona.edu (C.A. Bertulani).

0375-9474/$ – see front matter
doi:10.1016/j.nuclphysa.2005.12.014

of the type discussed here have already been successfully analyzed in the framework of Glauber's theory: in one-nucleon-removal reactions, the momentum distribution of the outgoing fragment has been shown to reflect the momentum distribution of the nucleon which is removed from the surface of the projectile nucleus [3]. However, because of complications involving multiple scattering processes in nucleus–nucleus collisions, a full Glauber multiple scattering expansion is impracticable. Fortunately, the study of many direct nuclear processes, e.g. nucleon knockout, or stripping, elastic breakup (diffraction dissociation), etc., are possible using the optical limit of the Glauber theory, in which the nuclear ground-state densities and the nucleon–nucleon total cross sections are the main input. In fact, this method has become one of the main tools in the study of nuclei far from stability [5]. When departures from the optical limit are observed, multiple nucleon–nucleon collisions and in-medium effects of the nucleon–nucleon interaction and nucleon–nucleon correlations become relevant.

Very peripheral collisions, with impact parameters just around the sum of the nuclear radii (grazing collisions), or larger, are well established tools for studying nuclear properties with intermediate energies and relativistic heavy ion collisions [6–8]. These collisions lead to excitation of giant resonances through both electromagnetic and strong interactions. At intermediate energy collisions ($E_{\rm lab} \simeq 100$ MeV/nucleon), or higher, the collision time is short and the action of the short-range nuclear interaction can excite the surface region of the colliding nuclei. This excitation can equilibrate forming a compound nucleus, and/or give rise to pre-equilibrium emission or other fast dissipation processes.

An interesting reaction mechanism in high-energy peripheral nucleus–nucleus collisions was suggested by Feshbach and Zabek [9,10]. This mechanism has been applied in Refs. [11–16] to the calculation of pion production in heavy ion collisions from subthreshold to relativistic energies. It is assumed that pions are produced in peripheral processes through the excitation of the projectiles to a Δ-isobar giant resonance. The results of these calculations were compared to inclusive pion production data for incident energies from 50 MeV to 2 GeV per nucleon. As emphasized by those authors, this comparison is not very meaningful at high energies where peripheral processes are expected to contribute very little to the total pion production. However, at subthreshold energies, coherent pion production should dominate the cross section. This mechanism is known as the nuclear Weizsäcker–Williams method. It works as follows.

The uncertainty relation associated to the variation of the time-dependent nuclear field on a scale Δz leads a relation between the energy, ΔE, and momentum transfer, Δp:

$$\Delta E \simeq \frac{\hbar}{\Delta t} = \frac{\hbar v}{\Delta z}, \qquad \Delta p \simeq \frac{\hbar}{\Delta z} \implies \Delta E = v \Delta p.$$

The last equation on the right is the dispersion relation of a phonon. For typical situations, Δz is a few fermi and the nuclear interaction pulse carries several hundred MeV. This relation can also be directly obtained from the collision kinematics. Let $(E_i, \mathbf{p}_i)$ be the initial momentum of the projectile and $(\Delta E, \Delta \mathbf{p})$ the energy–momentum transfer in the reaction. One has

$$\mathbf{P}_f = \mathbf{P}_i - \Delta \mathbf{p}, \qquad E_f = E_i - \Delta E.$$

From these relations one finds

$$\frac{\mathbf{P}_i \cdot \Delta \mathbf{p}}{E_i} - \Delta E = \frac{-(\Delta E)^2 + (\Delta p)^2 + (M_i^2 - M_f^2)c^4}{2E_i}.$$

Neglecting the term on the right-hand side, one gets

$$\Delta E = \mathbf{v} \cdot \Delta \mathbf{p} = v \Delta p_z, \tag{1}$$

where Δp_z is the momentum transfer along the longitudinal direction.

The above relation can only be satisfied for nuclear excitations of very small momentum transfers, even for moderately large energy transfers. This is the case for the excitation of giant resonances. Thus, the nuclear interaction in grazing nuclear collisions is an effective tool to probe giant resonances (for a review see, e.g., Ref. [17]). For very large impact parameters (larger than the sum of the nuclear density radii) only the electromagnetic interaction is present, and Eq. (1) (with $v \simeq c$) is just the energy–momentum relation of a real photon. In fact, relativistic Coulomb excitation is another useful tool for investigating giant resonances [6,8].

The phonon-like relation, Eq. (1), is also a tool for studying nucleon–nucleon short-range correlations. The energy in Eq. (1) could hardly be absorbed by a single nucleon since it would carry the momentum $\sim\sqrt{2m\Delta E}$, which is appreciably larger than that of Eq. (1). However, the phonon could be absorbed by a correlated nucleon pair, which can have large kinetic energy and small total momentum, when the nucleons move in approximately opposite directions. This mechanism has been exploited by previous authors to study the emission of correlated pairs in relativistic heavy ion collisions [25,26]. Remarkably, Refs. [9,10] do not treat properly the nuclear absorption at small impact parameters, leading to very large cross sections for the emission of correlated pairs in peripheral collisions.

In many-body physics the word correlation is used to indicate effects beyond mean-field theories. In nuclear physics one distinguishes between short- and long-range correlations. Nuclear collective phenomena such as vibrations and rotations are known to be ruled by long-range correlations. These effects are relatively well known. Short-range correlations is also a subject of intensive studies in nuclear physics (see, e.g., [18–23]). The sources of short-range correlations are the strong repulsive core of the microscopic nucleon–nucleon interaction at short internucleon distances. The nucleon–nucleon interaction becomes strongly repulsive at short distances. The phase shifts for $^1S_0$ and $^3S_1$ are positive at low, and become negative at higher energies [30]. This indicates a repulsive core at short distances and attraction at long distances. In the nuclear medium this repulsive interaction is strongly influenced by Pauli blocking. The search for nuclear phenomena showing short-range correlations effects is one of the most discussed topics in the nuclear structure community. For the nuclear reaction community, the importance of Pauli correlations in high energy nucleus–nucleus collisions has prompted the consideration of effects of dynamical short-range correlations. When one treats nucleus–nucleus collisions at high energies with an optical phase shift function one can include both the center-of-mass correlations and two-body correlations in a straightforward manner to obtain a rapidly converging series for the physical observables.

It would be proper at this time to look for fingerprints of short-range correlations in high-energy collisions involving rare nuclear isotopes. Recent experiments on knockout reactions seem to indicate a quenching of the spectroscopic factor relative to shell-model predictions in neutron-rich nuclei [5]. This reduction is thought to be a consequence of short-range correlations which spread the single particle strength to states with higher energies. In fact, systematic studies with the $A(e, e'p)$ reaction have provided ample evidence for this quenching phenomenon [24]. In this context, two-proton knockout reactions with exotic nuclear beams seem to be a promising tool to investigate short-range correlations in neutron- (proton-) rich nuclei [27]. Indeed, for decades two-proton knockout has been considered a valuable tool to study short-range correlations in proton–nucleus and electron–nucleus processes (for recent work, see, e.g., [22,23]). In high-energy nucleus–nucleus collisions, the phonon mechanism, proposed by Feshbach and Zabek, is a useful guide for the investigation of short-range correlations.

The plan of this paper is as follows. In this work I treat the effects of short-range correlations on heavy-ion scattering at high energies. In Section 2 the Glauber formalism for diffraction dissociation is reviewed. In Section 3 this formalism is shown to lead to the same result as the traditional DWBA calculations under the proper conditions. This is an important point, as diffraction dissociation and DWBA approaches are commonly referred to as distinct reaction mechanisms in the literature. In Section 4 the role of absorption and Lorentz boosts is discussed. In Section 5 the formalism is applied to heavy-ion collisions in the presence of two-body correlations, showing the connection with the Feshbach and Zabek method. The significance of short-range correlations is further discussed. In Section 6 the formalism is applied to carbon-carbon and $^{11}\mathrm{Li} + {}^{9}\mathrm{Be}$ collisions. In Section 7 some concluding remarks are made.

2. Diffraction dissociation

Let us consider high energy scattering, so that the energy transfer in the collision, ΔE, is much smaller than the kinetic energy of the colliding nuclei, E. In most cases, one is also interested in processes for which the fragments fly in the forward direction, i.e., we will also assume that $\Delta\theta \ll 1$. In such situations the particle wavefunctions are well described by eikonal waves [28], i.e., a plane wave distorted by an interaction, V, so that the S-matrix is given by the simple formula $S(b) = \exp[-(i/\hbar v)\int dZ\, V(R)]$, with v equal to the projectile velocity and $\mathbf{R} = (\mathbf{b}, Z)$ the distance between projectile and target (V is assumed to be spherically symmetric). Extending this approach to account for scattering of bound particles, the initial and final states are given by

$$\Psi_i = \phi_i(\mathbf{r}) \exp(i\mathbf{k}\cdot\mathbf{R}), \qquad \Psi_f = \phi_f(\mathbf{r}) S(b) \exp(i\mathbf{k}\cdot\mathbf{R}), \tag{2}$$

where $\phi_{i,f}(\mathbf{r})$ are the initial and final probability amplitudes (wavefunctions) that a particle in the projectile is at a distance $\mathbf{r}$ from the center of mass. The particle's S-matrix, $S(b)$, accounts for the distortion due to the interaction.

For a projectile with two-body structure (e.g., a core + valence particle)

$$\begin{aligned}\Psi_i &= \phi_i(\mathbf{r}) \exp\bigl[i(\mathbf{k}_c\cdot\mathbf{r}_c + \mathbf{k}_v\cdot\mathbf{r}_v)\bigr],\\ \Psi_f &= \phi_f(\mathbf{r}) S_c(b_c) S_v(b_v) \exp\bigl[i\bigl(\mathbf{k}'_c\cdot\mathbf{r}_c + \mathbf{k}'_v\cdot\mathbf{r}_v\bigr)\bigr],\end{aligned} \tag{3}$$

where now $\phi_{i,f}(\mathbf{r})$ are the initial and final intrinsic wavefunctions of the (core + valence particle) as a function of $\mathbf{r} = \mathbf{r}_1 - \mathbf{r}_2$. The relation between the intrinsic, $\mathbf{r}$, and center of mass, $\mathbf{R}$, coordinates is given in terms of the mass ratios $\beta_i = m_i/m_P$. Explicitly, $\mathbf{r}_v = \mathbf{R} + \beta_c\mathbf{r}$ and $\mathbf{r}_c = \mathbf{R} - \beta_v\mathbf{r}$. The core and valence particle S-matrices, $S_c(b_c)$ and $S_v(b_v)$, account for the distortion due to the interaction with the target.

The probability amplitude for diffraction dissociation is the overlap between the two wavefunctions above, i.e.,

$$A_{(\mathrm{diff})} = \int d^3r_c\, d^3r_v\, \phi_f^*(\mathbf{r})\phi_i(\mathbf{r})\delta(z_c + z_v) S_c(b_c) S_v(b_v) \exp\bigl[i(\mathbf{q}_c\cdot\mathbf{r}_c + \mathbf{q}_v\cdot\mathbf{r}_v)\bigr], \tag{4}$$

where $\mathbf{q}_c = \mathbf{k}'_c - \mathbf{k}_c$ is the momentum transfer to the core particle, and accordingly for the valence particle. The above formula yields the probability amplitude that the projectile starts the collision in a bound state and ends up as two separated pieces. The S-matrices, S_c and S_v carry all the information about the dissociation mechanism. The delta-function $\delta(Z)$ in Eq. (4) was introduced to account for the fact that the S-matrices calculated in the eikonal approximation only depend on the transverse direction.

It is instructive to follow another argument to obtain Eq. (4). If only the core scatters elastically, whereas the valence particle remains in its unaltered plane wave state, the final projectile wavefunction is given by

$$\Psi_f^{(\text{scatt})} = \phi_f(\mathbf{r})\big[1 - S_c(b_c)\big]\exp\big[i\left(\mathbf{k}'_c \cdot \mathbf{r}_c + \mathbf{k}'_v \cdot \mathbf{r}_v\right)\big]. \tag{5}$$

The factor $[1 - S_c(b_c)]$ is the amplitude for elastic scattering of the core. The same relation can be applied for the valence particle. The diffraction dissociation occurs by subtracting the simultaneous scattering of the core + valence particle, represented by $[1 - S_c(b_c)][1 - S_v(b_v)]$, from the independent scattering of core and the valence particle, i.e.,

$$\begin{aligned}\hat{S}_{(\text{diff})} &= \big[1 - S_c(b_c)\big]\big[1 - S_v(b_v)\big] - \big[1 - S_c(b_c)\big] - \big[1 - S_v(b_v)\big] \\ &= S_c(b_c)S_v(b_v) - 1.\end{aligned} \tag{6}$$

The factor (-1) is not relevant because of the orthogonality of the wavefunctions $\phi_i(\mathbf{r})$ and $\phi_f(\mathbf{r})$. Using $A_{(\text{diff})} = \langle \phi_i \varphi_{\mathbf{k}_1,\mathbf{k}_2} | \hat{S}_{(\text{diff})} | \phi_f \varphi_{\mathbf{k}'_1,\mathbf{k}'_2} \rangle$, with $\varphi_{\mathbf{k}_1,\mathbf{k}_2}$ equal to plane waves, we regain Eq. (4). We thus see that diffractive dissociation (or elastic nuclear breakup) arises from the momentum transfer to each particle due to elastic scattering, subtracting the momentum transfer to their center of mass.

The cross section for the diffraction process $\phi_i(\mathbf{r}) \to \phi_f(\mathbf{r})$ is given by

$$d\sigma = \rho(E)\left|\int d^3r_c\, d^3r_v\, \phi_f^*(\mathbf{r})\phi_i(\mathbf{r})\delta(z_c + z_v)S_c(b_c)S_v(b_v)\exp\big[i\left(\mathbf{q}_c \cdot \mathbf{r}_c + \mathbf{q}_v \cdot \mathbf{r}_v\right)\big]\right|^2, \tag{7}$$

where $\rho(E)$is the density of final states, $\rho(E) = \delta(Q_z)\, d^3q_c\, d^3q_v/(2\pi)^5$, where $\mathbf{Q} = \mathbf{q}_c + \mathbf{q}_v$ is the momentum transfer to the center of mass of the projectile. The delta function accounts for the conservation of the longitudinal momentum of the projectile arising from the use of eikonal wavefunctions (i.e., no dependence on the longitudinal c.m. scattering).

It is important to notice that the above formula is somewhat different than Eq. (8) of Ref. [29]. In that reference the coordinates $\mathbf{r}$, $\mathbf{R}$ were used from the start. One can transform the integral of Eq. (7) to those variables. The Jacobian of the transformation is equal to one and $d^3r_c\, d^3r_v = d^3r\, d^3R$, $d^3q_c\, d^3q_v = d^3q\, d^3Q$, where $\mathbf{q} = \beta_c\mathbf{q}_v - \beta_v\mathbf{q}_c$ is the momentum transfer to the intrinsic coordinates of the projectile. Thus, in the coordinates $\mathbf{r}$, $\mathbf{R}$, Eq. (7) reduces to

$$d\sigma = \frac{d^3q\, d^2Q}{(2\pi)^5}\left|\int d^3r\, d^2b\, \phi_f^*(\mathbf{r})\phi_i(\mathbf{r})S_c(b_c)S_v(b_v)\exp\big[i\left(\mathbf{q}\cdot\mathbf{r} + \mathbf{Q}\cdot\mathbf{b}\right)\big]\right|^2. \tag{8}$$

The above formula reduces to Eq. (8) of Ref. [29] if one sets $\beta_v = 1$ and $\beta_c = 0$. In this equation, $\phi_f(\mathbf{r})$ can be taken as any final state of the projectile. Thus, it is not only appropriate to calculate *diffraction dissociation*, but also *diffraction excitation*. Diffraction excitation occurs when the final state $\phi_f(\mathbf{r})$ is a bound state. If it is a state in the continuum (diffraction dissociation), then $\phi_f(\mathbf{r})$ should be set to the unity,[1] since the part of the wavefunction given by $S_cS_v\exp[i(\mathbf{k}'_c \cdot \mathbf{r}_c + \mathbf{k}'_v \cdot \mathbf{r}_v)]$ already accounts for the proper wavefunction of the projectile. A natural improvement of Eq. (7) is to include final state interactions between the core and the valence particle in the coordinate dependence of $\phi_f(\mathbf{r})$.

[1] Neglecting final state interactions. If final state interactions are important, $\phi_f(\mathbf{r})$ is the distortion correction to the plane wave.

Since I claim here that Eq. (8) can also be used for calculating excitation cross sections, it is adequate to show the relation of this approach to the traditional DWBA and semiclassical methods for nuclear excitation in nucleus–nucleus collisions. We will see that the latter are perturbative expansions of the Eq. (8).

3. DWBA and semiclassical methods

On can factorize the S-matrices defined in Section 2 for the interaction of the core and valence particle with the target in terms of their phase-shifts

$$\chi = -\frac{1}{\hbar v}\int_{-\infty}^{\infty} dZ\, V(R). \tag{9}$$

In the weak interaction limit, or perturbation limit, the phase-shifts are very small so that

$$\begin{aligned} S_c(b_c)S_v(b_v) &= \exp\bigl[i(\chi_c+\chi_v)\bigr] \simeq 1 + i\chi_c + i\chi_v \\ &= 1 - \frac{i}{\hbar v}\int V_{cT}(\mathbf{r}_c)\,dz_c - \frac{i}{\hbar v}\int V_{vT}(\mathbf{r}_v)\,dz_v. \end{aligned} \tag{10}$$

The factor 1 does not contribute to the breakup**.** Thus, inserting the result above in Eq. (4), one obtains

$$A_{(\mathrm{PWBA})} \simeq \frac{1}{i\hbar v}\int d^3r_c\, d^3r_v\, \phi_f^*(\mathbf{r})\phi_i(\mathbf{r})\bigl[V_{cT}(\mathbf{r}_c)+V_{vT}(\mathbf{r}_v)\bigr]\exp\bigl[i(\mathbf{q}_c\cdot\mathbf{r}_c+\mathbf{q}_v\cdot\mathbf{r}_v)\bigr], \tag{11}$$

where the integrals over z_c and z_v in Eq. (10) were absorbed back to the integrals over $\mathbf{r}_c$ and $\mathbf{r}_v$ after use of the delta-function $\delta(z_c+z_v)$. The above equation is nothing more than the plane-wave Born-approximation (PWBA) amplitude. However, absorption is not treated properly. For small values of $\mathbf{r}_c$ and $\mathbf{r}_v$ the phase-shifts are not small and the approximation used in Eq. (10) fails. A better approximation is to assume that for small distances, where absorption is important, $S_c(b_c)S_v(b_v) \simeq S(b)$, where the right-hand side is the S-matrix for the projectile scattering as a whole on the target. Using the coordinates $\mathbf{r}$ and $\mathbf{R}$, and defining $U_{\mathrm{int}}(\mathbf{r},\mathbf{R}) = V_{cT}(\mathbf{r}_c)+V_{nT}(\mathbf{r}_n)$, one gets

$$\begin{aligned} T_{(\mathrm{DWBA})} &= i\hbar v A_{(\mathrm{DWBA})} \\ &\simeq \int d^3r\, d^3R\, \phi_f^*(\mathbf{r})\exp[i\mathbf{q}\cdot\mathbf{r}]\phi_i(\mathbf{r})U_{\mathrm{int}}(\mathbf{r},\mathbf{R})S(b)\exp[i\mathbf{Q}\cdot\mathbf{R}]. \end{aligned} \tag{12}$$

In elastic scattering, or excitation of collective modes (e.g., giant resonances), the momentum transfer to the intrinsic coordinates can be neglected and the equation above can be written as

$$T_{(\mathrm{DWBA})} = \bigl\langle \chi^{(-)}(\mathbf{R})\phi_f(\mathbf{r})\bigl|U_{\mathrm{int}}(\mathbf{r},\mathbf{R})\bigr|\chi^{(+)}(\mathbf{R})\phi_i(\mathbf{r})\bigr\rangle, \tag{13}$$

which has the known form of the DWBA T-matrix. The scattering phase space now only depends on the center of mass momentum transfer $\mathbf{Q}$. When the center of mass scattering waves are represented by eikonal wavefunctions, one has

$$\chi^{(-)*}(\mathbf{R})\chi^{(+)}(\mathbf{R}) \simeq S(b)\exp[i\mathbf{Q}\cdot\mathbf{R}]. \tag{14}$$

This shows that the PWBA and the DWBA are perturbative expansions of the diffraction dissociation formula (4).

In DWBA (or in the eikonal approximation, Eq. (14)), b does not have the classical meaning of an impact parameter. To obtain the semiclassical limit one goes one step further. By using Eq. (12) and assuming that R depends on time so that $R = (\mathbf{b}, z = vt)$, the semiclassical scattering amplitude is given by $A^{(i\to f)}_{(\text{semiclass})} = \int d^2b\, a^{(i\to f)}_{(\text{semiclass})}(b) \exp(i\mathbf{Q}\cdot\mathbf{b})$, where

$$a^{(i\to f)}_{(\text{semiclass})}(b) = \frac{1}{i\hbar} S(b) \int dt\, d^3r \exp(i\omega_{if}t)\phi^*_f(\mathbf{r}) U_{\text{int}}(\mathbf{r},t)\phi_i(\mathbf{r}), \tag{15}$$

where Eq. (1) was used ($Q_z Z = \omega_{if} t$).

The semiclassical probability for the transition $(i \to f)$ is obtained from the above equation after squaring and integrating it over $\mathbf{Q}$. One gets $\sigma^{(i\to f)} = \int d^2b\, P^{(i\to f)}_{(\text{semiclass})}(b)$, where $P^{(i\to f)}_{(\text{semiclass})}(b) = |a^{(i\to f)}_{(\text{semiclass})}(b)|^2$, with b having now the explicit meaning of an impact parameter. Thus, $a^{(i\to f)}_{(\text{semiclass})}(b)$, is the semiclassical excitation amplitude. Eq. (15) is well known (for example, in Coulomb excitation at low energies) except that the factor $S(b)$ is usually set to one. In high energy collisions it is crucial to keep this factor, as it accounts for refraction and absorption at small impact parameters: $|S(b)|^2 = \exp[2i\chi^{(\text{imag})}]$, where $\chi^{(\text{imag})}$ is calculated with the imaginary part of the optical potential. The derivation of the DWBA and semiclassical limits of eikonal methods can be easily extended to higher orders in the perturbation V. The eikonal method includes all terms of the perturbation series in the sudden-collision limit.

4. Role of absorption and of Lorentz boosts

At this point it is interesting to consider the calculation performed by Feshbach and Zabek [9]. In that work, Eq. (15), or its equivalent PWBA form, Eq. (11), without a proper account of the strong absorption at small impact parameters (described in Eq. (15) by $S(b)$), was used to calculate the total cross section for emission of a correlated nucleon pair in peripheral collisions with heavy ions. Also, interactions without imaginary parts were used. As a consequence, they found extremely large cross sections; $\sim$1 barn for $^{16}\text{O} + {}^{16}\text{O}$ collisions at energies $\sim$1 GeV/nucleon. This is certainly inconsistent with perturbation theory. As seen schematically in Fig. 1, the product of the S-matrix and the interaction potential implies that the reaction occurs in a narrow region at "grazing" impact parameters. The width of this region is approximately $\Delta \simeq 1$–2 fm. The cross section might be written as $\sigma \simeq 2\pi\Delta(R_P + R_T)P$, where P is the average probability

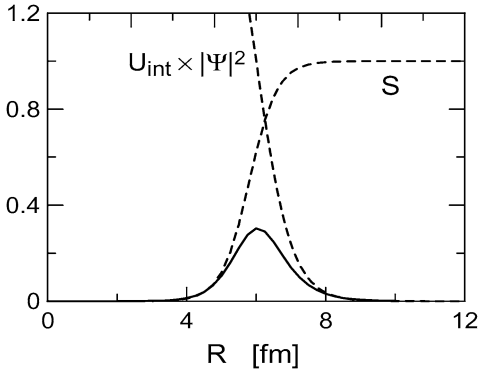

Fig. 1. Schematic diagram showing how the product of the S-matrix and the interaction potential (weighted by the wavefunction) would limit the cross section to grazing impact parameters.

for this reaction to occur within the impact parameter interval Δ, and R_P (R_T) is the projectile (target) radius. For light nuclei $2\pi\Delta(R_P + R_T) \simeq 300$–$600$ mb. Thus, the probability P violates unitarity (perturbation theory is invalid) if cross sections of the order of 1 barn are obtained.

Ref. [9] also introduced relativistic corrections to the nuclear potential. This relativistic property is most easily seen within a folding potential model for a nucleon–nucleus collision:

$$V(\mathbf{r}) = \int dr'^3 \rho_T(\mathbf{r}') v_{NN}(\mathbf{r} - \mathbf{r}'), \tag{16}$$

where $\rho_T(\mathbf{r}')$ is the nuclear density of the target. In the frame of reference of the projectile, the density of the target looks contracted and particle number conservation leads to the relativistic modification of Eq. (16) so that $\rho_T(\mathbf{r}') \to \gamma\rho_T(\mathbf{r}'_\perp, \gamma z')$, where $\mathbf{r}'_\perp$ is the transverse component of $\mathbf{r}'$ and $\gamma = (1 - v^2/c^2)^{-1/2}$ is the Lorentz contraction factor, with v equal to the relative velocity of projectile and target. But the number of nucleons as seen by the target (or projectile) per unit area remains the same. In other words, a change of variables $z'' = \gamma z'$ in the integral of Eq. (16) seems to restore the same Eq. (16). However, this change of variables also modifies the nucleon–nucleon interaction $v_{\rm NN}$. Thus, relativity introduces non-trivial effects in a potential model description of nucleus–nucleus scattering at high energies.

Colloquially speaking, nucleus–nucleus scattering at high energies is not simply an incoherent sequence of nucleon–nucleon collisions. Since the nucleons are confined within a box (inside the nucleus), Lorentz contraction induces a collective effect: in the extreme limit $\gamma \to \infty$ all nucleons would interact at once with the projectile. This is often neglected in pure geometrical (Glauber model) descriptions of nucleus–nucleus collisions at high energies, as it is assumed that the nucleons inside "firetubes" scatter independently.

Assuming that the nucleon–nucleon interaction is of very short range so that the approximation $v_{\rm NN}(\mathbf{r} - \mathbf{r}') = J_0\delta(\mathbf{r} - \mathbf{r}')$ can be used, one sees from Eq. (16) that $V(\mathbf{r})$, the interaction that a nucleon in the projectile has with the target nucleus, also has similar transformation properties as the density: $V(\mathbf{r}) \to \gamma V(\mathbf{r}_\perp, \gamma z)$, i.e., $V(\mathbf{r})$ transforms as the time-component of a four-vector. In this situation, the Lorentz contraction has no effect whatsoever in the diffraction dissociation amplitudes, described in the previous sections within the eikonal approximation. This is because a change of variables $Z' = \gamma Z$ in the eikonal phases leads to the same result as in the non-relativistic case, as can be easily checked from Eq. (9). Of course, the delta-function approximation for the nucleon–nucleon interaction means that nucleons will scatter at once, and Lorentz contraction does not introduce any additional collective effect. This is not the case for realistic interactions with finite range. Thus, nuclear structure studied with high-energy nucleus–nucleus collisions is immensely complicated by retardation effects and is not well understood.

5. Emission of correlated pairs in peripheral reactions

Lets us now consider the emission of correlated pairs in peripheral collisions. The projectile is now a three-body system, with notation for the coordinates as shown in Fig. 2. Following the same arguments used in Section 2, the wavefunction of a three-body projectile in the initial and final states is given by

$$\begin{aligned}
\Psi_i &= \phi_i(\mathbf{r}_1, \mathbf{r}_2) \exp\bigl[i(\mathbf{K}_c \cdot \mathbf{r}_c + \mathbf{k}_1 \cdot \mathbf{r}_1 + \mathbf{k}_2 \cdot \mathbf{r}_2)\bigr], \\
\Psi_f &= \phi_f(\mathbf{r}_1, \mathbf{r}_2) S_c(b_c) S_1(b_1) S_2(b_2) \exp\bigl[i(\mathbf{K}'_c \cdot \mathbf{r}_c + \mathbf{k}'_1 \cdot \mathbf{r}_1 + \mathbf{k}'_2 \cdot \mathbf{r}_2)\bigr],
\end{aligned} \tag{17}$$

where now $\phi_{i,f}(\mathbf{r}_1, \mathbf{r}_2)$ are the initial and final intrinsic wavefunctions of the correlated nucleon–nucleon pair as a function of their intrinsic coordinates $\mathbf{r}_1$, $\mathbf{r}_2$. Assuming that the nucleon mass

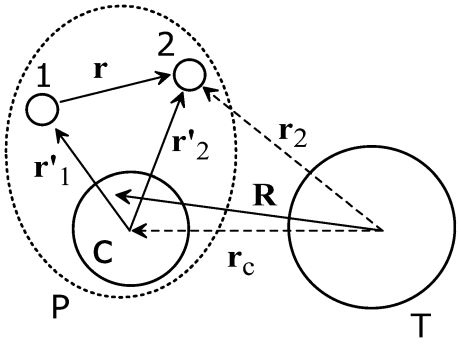

Fig. 2. Coordinates used in text for the three-body projectile interacting with the target. The coordinate $\mathbf{r}_1$ is not shown for simplicity.

is much smaller than that of the core, one can replace $\mathbf{r}_c \simeq \mathbf{R}$, where $\mathbf{R}$ is the center of mass of the projectile.

Following the same steps as before, a relation similar to Eq. (8) can be obtained for the cross section for the energy absorption by a correlated pair (when final state interactions are neglected):

$$d\sigma = \frac{d^3q_1\, d^3q_2\, d^2Q}{(2\pi)^8} \times \left| \int d^3r_1\, d^3r_2\, d^2b\, \phi_f^*(\mathbf{r}_1,\mathbf{r}_2)\phi_i(\mathbf{r}_1,\mathbf{r}_2) S(b) S_1(b_1) S_2(b_2) \times \exp\bigl[i(\mathbf{q}_1\cdot\mathbf{r}_1 + \mathbf{q}_2\cdot\mathbf{r}_2 + \mathbf{Q}\cdot\mathbf{b})\bigr] \right|^2, \tag{18}$$

where $\mathbf{Q} = \mathbf{K}'_c - \mathbf{K}_c$. If the intrinsic nucleon coordinates are denoted by $\mathbf{r}'_i = \mathbf{r}_i - \mathbf{R}$, one has $b_i = \sqrt{b^2 + r_i^2 \sin^2\theta_i + 2r_i b \sin\theta_i \cos(\phi - \phi_i)}$.

The above relation can be used for the emission of the nucleon pair. Neglecting final state interactions and assuming that the core is not observed (i.e., integrating over $\mathbf{Q}$), one gets

$$d\sigma = \frac{d^3q_1\, d^3q_2}{(2\pi)^6} \int d^2b \left|S(b)\right|^2 \times \left| \int d^3r_1\, d^3r_2\, \phi_i(\mathbf{r}_1,\mathbf{r}_2) S_1(b_1) S_2(b_2) \exp\bigl[i(\mathbf{q}_1\cdot\mathbf{r}_1 + \mathbf{q}_2\cdot\mathbf{r}_2)\bigr] \right|^2. \tag{19}$$

In order to proceed further one needs a model wavefunction for the correlated pair, $\phi_i(\mathbf{r}_n, \mathbf{r}_{n'})$. The wavefunction used will have the form

$$\phi_i(\mathbf{r}_1,\mathbf{r}_2) = \phi_\alpha(\mathbf{r}_1)\phi_\beta(\mathbf{r}_2) f_{\rm corr}(\mathbf{r},\mathbf{r}_c), \tag{20}$$

where $\mathbf{r} = \mathbf{r}_1 - \mathbf{r}_2$, $\phi_\alpha(\mathbf{r}) = \phi_{nljm}(\mathbf{r})$ are single particle wavefunctions with quantum numbers $\alpha = nljm$, and $f_{\rm corr}(\mathbf{r},\mathbf{r}_c)$ is a function for the nucleon pair distance $\mathbf{r}$, which also depends on a two-particle correlation parameter $\mathbf{r}_c$ so that $f_{\rm corr}(\mathbf{r},\mathbf{r}_c) \to 0$ as $\mathbf{r}_c \to 0$. The effective correlation function $f_{\rm corr}(\mathbf{r},\mathbf{r}_c)$, the so-called Jastrow factor [32], is a statistical average of the Pauli correlation function [31] and the correlation function for the dynamical short-range (e.g., hard core) correlation.

As argued in Ref. [33], the true ground-state wave function of the nucleus containing correlations coincide with the independent particle, or Hartree–Fock wavefunction, for interparticle distances $r \geqslant r_{\rm heal}$, where $r_{\rm heal} \simeq 1$ fm is the so-called "healing distance". This behavior is a consequence of the constraints imposed by the Pauli principle. Nucleons are kept apart at short distances, while for distances beyond several K_F^{-1}'s there is little effect. Consequently, nucleon–nucleon collisions at short distances are rare in nuclear matter, and because the strongest part of the interaction is at short distances, the effective force between the nucleons is much less than in free space. For example, if a nucleon in ^{16}O felt the cumulative sum of 16 nucleon–nucleon potentials, it would feel a potential of ∼1400 MeV; yet empirically it is known that the effective potential felt by the nucleon in the middle of the nucleus is only ∼40–50 MeV deep.

Although, in general, the correlation function $f_{\rm corr}(\mathbf{r}, \mathbf{r}_c)$ may depend on the isospin and spin quantum numbers of the two-body channel, we will assume for simplicity that it is a plain, state independent, Jastrow factor [32]. The effects of nucleon–nucleon correlations in nucleus–nucleus collisions have also been studied in several works. For example, in Ref. [34] short-range correlations were shown to play an important role in nucleon–nucleus collisions at intermediate and high energies.

The two-particle correlation distance, $\mathbf{r}_c$, is a combination of four contributions [34]

$$r_c = r_{\rm Pauli} + r_{\rm SRD} + r_{\rm PSR} + r_{\rm CM}, \tag{21}$$

where $r_{\rm Pauli}$ is due to Pauli exclusion-principle correlations, $r_{\rm SRD}$ is related to short-range dynamical correlations, $r_{\rm PSR}$ is due to a combination of the Pauli and the short-range dynamical term, and $r_{\rm CM}$ is due to center-of-mass correlations [35]. An approximate set of expressions for each of these terms is given by

$$\begin{aligned}
r_{\rm Pauli} &= \frac{1}{2}\left(1 - \frac{5}{A} + \frac{4}{A^2}\right)\frac{3\pi}{10K_F}\frac{1}{1+\frac{8}{5}BK_F^2}, \\
r_{\rm SRD} &= \frac{1}{2}\left(1 - \frac{2}{A} + \frac{1}{A^2}\right)\sqrt{\pi}\frac{b^3}{b^2+8B}, \\
r_{\rm PSR} &= \frac{1}{2}\left(1 - \frac{5}{A} + \frac{4}{A^2}\right)\frac{3\pi}{10}\left(K_F^2 + \frac{5}{b^2}\right)^{-1/2}\left[1 + 8B\left(\frac{K_F^2}{5} + \frac{1}{b^2}\right)\right]^{-1}, \\
r_{\rm CM} &= \left(1 - \frac{2}{A} + \frac{1}{A^2}\right)l_c,
\end{aligned} \tag{22}$$

where A and $K_F = (1.5\pi^2\rho)^{1/3} \simeq 1.36$ fm^{-1} are the target number and the Fermi momentum of the target nucleus, respectively. b is a short-range dynamical correlation, $b \simeq 0.4$ fm, B is the finite-range parameter of the nucleon–nucleon elastic t-matrix, $B \simeq 0.62$ fm^2 (for collisions around 200 MeV/nucleon), and l_c is the effective "correlation length", $l_c \simeq 1.3A^{-5/6}$ fm. For proton + ^{12}C collisions at 200 MeV/nucleon this set of parameters yields, $r_{\rm Pauli} \simeq 0.3$ fm, $r_{\rm SRD} \simeq 0.01$ fm, $r_{\rm PSR} \simeq 0.0016$ fm, $r_{\rm CM} \simeq 0.18$ fm, and $r_c \simeq 0.5$ fm. This in fact overestimates the correlation distance. A more detailed calculation, using the parameters B, b and l_c from Ref. [34] shows that r_c has an appreciable dependence on the collision energy, as shown in Fig. 3 for protons incident on ^{12}C. Thus, in nuclear reactions, r_c can vary substantially with the collision energy and with mass numbers.

The estimates done above show that the main contribution to the correlation distance arises from the Pauli principle. Let us assume a correlation function of the form

$$f_{\rm corr}(r) = 1 - \exp\left[-\frac{(\mathbf{r}_1 - \mathbf{r}_2)^2}{r_c^2}\right]. \tag{23}$$

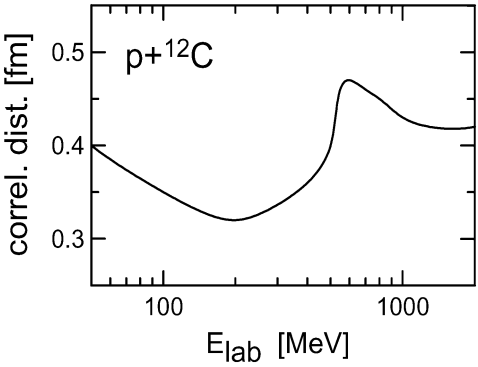

Fig. 3. Dependence of the short-range correlation distance, r_c, on the proton energy in the reaction $p + {}^{12}C$.

This correlation function implies that the pair wavefunction decreases for small relative distances, $r = |\mathbf{r}_1 - \mathbf{r}_2| \lesssim r_c$. The correlation function $f_{\rm corr}(\mathbf{r}, \mathrm{r}_c)$ goes to one for large values of r and to zero for $r \to 0$. In nuclear structure calculations, the effect of correlation, introduced by the function $f_{\rm corr}(\mathbf{r}, \mathrm{r}_c)$, becomes large when the correlation distance parameter r_c becomes large, and vice versa. Here, only the effects of short-range correlations are studied and it would be manifest in momentum distributions of highly energetic nucleons, as discussed in the introduction, and explicitly shown in the next section. It is important to notice that the Gaussian correlation function, Eq. (23), is unrealistic. Indeed, the short-range repulsion is at the origin of the decrease of the pair wavefunction for small relative distances. At the same time, there will be an increased probability to find the nucleon pair at medium internucleon distances. A two-Gaussian parameterization is needed to quantify this well-known effect of short-range correlations. For simplicity, only the simple parameterization of Eq. (23) is used in this work.

Inserting Eqs. (20) and (23) in Eq. (19) and integrating over the pair momenta, one gets

$$\sigma_{\rm SR} = \frac{(C^2S)_{lj}(C^2S)_{l'j'}}{(2j+1)(2j'+1)} \sum_{m,m'} \int d^2b \left|S(b)\right|^2 \times \int d^3r_1\, d^3r_2 \left|\phi_{nljm}(\mathbf{r}_1) S_1(b_1) \phi_{n'l'j'm'}(\mathbf{r}_2) S_2(b_2) f_{\rm corr}(\mathbf{r}, \mathrm{r}_c)\right|^2. \tag{24}$$

The cross section has been averaged over the initial magnetic quantum numbers of the nucleons. If the correlation function were equal to the unity, the integrand would be the product of the probabilities to remove an uncorrelated nucleon, with quantum numbers $nljm$. The later probability is given by $\int d^3r\, |\phi_{nljm}(\mathbf{r}) S_i(b)|^2$.

The spectroscopic factors in Eq. (24) have a complex dependence on the angular momenta of the nucleon pair. The correlations arising from angular momentum coupling have been studied in Ref. [37]. Here we will assume a simple combinatorics so that $(C^2S)_{lj} = n(n-1)/2$, where n is the number of nucleons in the valence shell.

We see from the equations above that the cross section for the emission of a correlated pair is smaller than that for the emission of independent particles, since $f_{\rm corr}(\mathbf{r}, \mathbf{r}_c) \leqslant 1$. Most part of the integrand will have $f_{\rm corr}(\mathbf{r}, \mathbf{r}_c) \sim 1$, except for the small region of volume $\mathcal{N} r_c^3$, where $\mathcal{N}$ is a number of order of one. Conservative estimates (using $r_c = 0.3$–1 fm), imply that the cross section for emission of a correlated pair could not exceed 100 mb, in contrast to the results obtained in Refs. [9,10]. I will show this for specific reactions in the following section.

6. Results and discussions

The numerical calculations have been carried out for the systems $^{12}C + {}^{12}C$ at 250 MeV/nucleon and $^{11}Li + {}^{9}Be$ at 287 MeV/nucleon. In both cases, there are some experimental data available for two-nucleon removal. This also allows for the study of the influence of a halo wavefunction (^{11}Li) in the results. The wavefunctions were calculated by using a Woods–Saxon potential with a spin-orbit and Coulomb potential,

$$V(r) = U_r(r) + U_s(r) + U_C(r), \tag{25}$$

where

$$U_r(r) = V_r\left(1 + e^{\rho_r}\right)^{-1}, \qquad U_s(r) = V_s(\mathbf{l}\cdot\mathbf{s})\frac{(2\ \text{fm}^2)}{r}\frac{d}{dr}\left(1 + e^{\rho_s}\right)^{-1}, \tag{26}$$

$U_C(r)$ is the potential for a uniformly charged sphere with charge $Z - 1$ (0, for neutrons) and radius R_C, and $\rho_i = (r - R_i)/a_i$.

For protons in the $1p_{3/2}$ orbital of ^{12}C the separation energy is 15.96 MeV (the two-proton separation energy is 27.18 MeV), which can be reproduced with the parameters $V_r = -57.41$ MeV, $V_s = -6.0$ MeV, $R_r = R_C = R_s = 3.011$ fm, $a_r = 0.52$ fm and $a_s = 0.65$ fm.

The reactions and structure of the two-neutron halo nucleus ^{11}Li have attracted much interest. It is a Borromean system in the sense that although the three-body system, consisting of ^{9}Li and two neutrons, forms a bound state, none of the possible two-body subsystems have bound states. Hence the stability of ^{11}Li is brought about by the interplay of the core–neutron and the neutron–neutron interactions, which must lead to a strongly correlated wave function with the two neutrons spatially close together. For the calculation here we will approximate the ^{11}Li ground state by an inert ^{9}Li core coupled to a neutron pair in a $(2s\frac{1}{2})^2$ state, although the most probable configuration is an admixture of neutron pairs in $(2s\frac{1}{2})^2$, $(1p\frac{1}{2})^2$, and $(1d\frac{5}{2})^2$ states [38,39]. However, the former assumption allows for a simpler calculation of the correlated-pair emission. The potential parameters are adjusted to obtain the single-particle wave functions, reproducing the effective neutron separation energies. The two-neutron separation energy is 0.3 MeV. From the systematics in Fig. 6 of [40], the estimated ^{10}Li average excitation energies is 0.2 MeV for the single-particle state. Taking this value for two-neutron coupling to the ^{9}Li core, one arrives at an effective neutron separation energy of 0.5 MeV. This binding energy for the $n + {}^{10}$Li system can be reproduced with the potential parameters $V_r = -42.93$ MeV, $V_s = -6.0$ MeV, $R_r = R_C = R_s = 3.25$ fm and $a_r = a_s = 0.65$ fm.

The single-particle wavefunctions obtained in this way were used in Eq. (19) to calculate the momentum distributions of the correlated pair. The integrals in Eq. (24) were performed using a method similar to that described in the appendix of Ref. [39]. The S-matrices (and optical potentials) were calculated by using the "t–$\rho\rho$" interaction, as described in Refs. [34,36]. This is the same approximation used in Ref. [5].

In heavy ion physics it is common to define a correlation function by means of

$$C(\mathbf{q}_1, \mathbf{q}_2) = \left(\frac{d\sigma}{d^3q_1\, d^3q_2}\right) \Big/ \left(\frac{1}{\sigma}\frac{d\sigma}{d^3q_1}\frac{d\sigma}{d^3q_2}\right), \tag{27}$$

where the cross sections in the denominator are for the emission of a single nucleon. An accurate measurement of r_c requires the measurement of this correlation function for back-to-back (or nearly) pair emission. Until now, heavy ion data refer mainly to small relative momentum transfers. Data would only be interesting for the present purposes if the triggering conditions

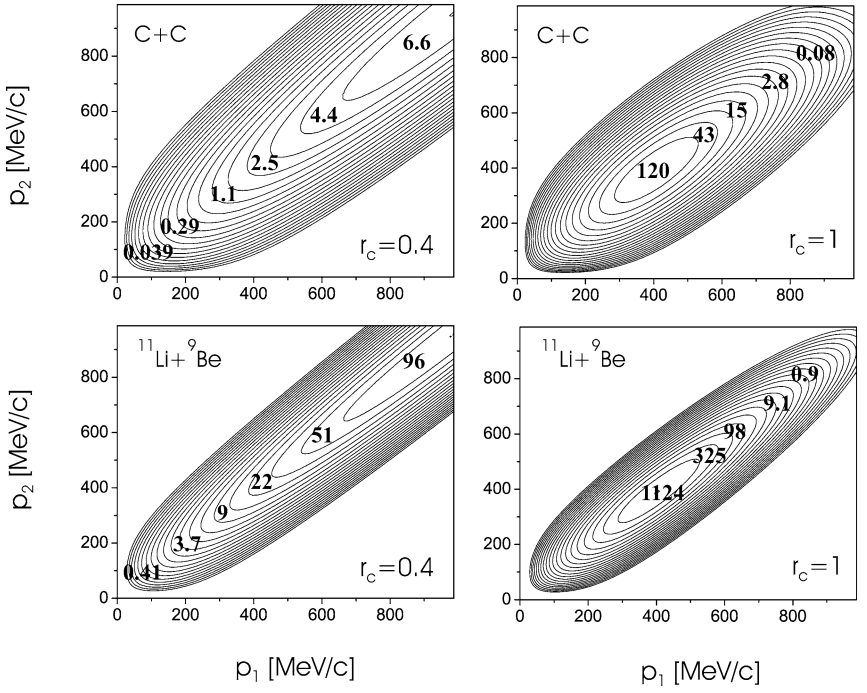

Fig. 4. Contour plots of $d\sigma/dq_1\,dq_2$ for the collision $^{12}\mathrm{C} + {}^{12}\mathrm{C}$ at 250 MeV/nucleon (upper panels) and $^{11}\mathrm{Li} + {}^{9}\mathrm{Be}$ at 287 MeV/nucleon (lower panels), as a function of $p_1 = \hbar q_1$ and $p_2 = \hbar q_2$. The left (right) panels are for $r_c = 0.4$ (1) fm. The numbers in the plots indicate the cross section, $d\sigma/dq_1\,dq_2$, in units of 10^{-5} [mb/(MeV/c)]^2.

were changed and if special attention was paid to back-to-back emission. In the present work, $d\sigma/dq_1\,dq_2$, instead of $C(\mathbf{q}_1, \mathbf{q}_2)$, will be used for the study of emission of correlated nucleons.

In Fig. 4 contour plots for $d\sigma/dq_1\,dq_2$ are presented for the collision $^{12}\mathrm{C} + {}^{12}\mathrm{C}$ at 250 MeV/nucleon and $^{11}\mathrm{Li} + {}^{9}\mathrm{Be}$ at 287 MeV/nucleon, as a function of $p_1 = \hbar q_1$ and $p_2 = \hbar q_2$. The nucleons are assumed to be emitted back-to-back, the nucleon 1 at 0° and nucleon 2 at 180° with respect to the beam axis, respectively. The upper panels are for the C + C collision, while the lower panels are for the Li + Be collisions. The left (right) panels are for $r_c = 0.4$ fm ($r_c = 1$ fm). The numbers in the plot indicate the cross section, $d\sigma/dq_1\,dq_2$, in units of 10^{-5} [mb/(MeV/c)]^2. One notices a strong correlation between the nucleon momenta, resulting from the phonon relationship, Eq. (1). The effect of the phonon dispersion relation is to produce a ridge in the cross section.

To obtain a greater physical insight, I will now use the PWBA approximation as in Eq. (12) (with $S(b) = 1$), so that, instead of the integrals in Eq. (19), one needs now to calculate

$$T_{(\mathrm{PWBA})} = \int d^3r_1\, d^3r_2\, \phi_i(\mathbf{r}_1, \mathbf{r}_2)\big[V_1(\mathbf{r}_1) + V_2(\mathbf{r}_2)\big] \exp\big[i(\mathbf{q}_1 \cdot \mathbf{r}_1 + \mathbf{q}_2 \cdot \mathbf{r}_2)\big]. \tag{28}$$

Let us assume that the potentials $V_{1,2}$ are given by Gaussian functions, i.e., $V_{1,2} = V_{1,2}^{(0)} \times \exp(-r_{1,2}^2/\lambda^2)$ and similarly for the wavefunctions, i.e., $\phi_{\alpha,\beta} = N \exp(-r_{1,2}^2/\Delta^2)$. In this case it is straightforward to perform analytically all the integrals in Eq. (28). If one further assumes that the correlation distance, r_c, is much smaller than the dimensions of the uncorrelated wavefunctions and of the potential, i.e., if $r_c \ll \Delta, \lambda$, one gets

$$T_{(\mathrm{PWBA})} = \left(V_1^{(0)} + V_2^{(0)}\right) \frac{(\pi N^2 r_c \Delta/\sqrt{\mathcal{A}})^3}{8} \left[\exp\left(-\frac{q_1^2 r_c^2}{4}\right) + \exp\left(-\frac{q_2^2 r_c^2}{4}\right)\right] \times \exp\left[-\frac{\Delta^2}{16\mathcal{A}}|\mathbf{q}_{1\perp} + \mathbf{q}_{2\perp}|^2\right] \exp\left[-\frac{\Delta^2}{16\mathcal{A}}\left(q_{1z} + q_{2z} - \frac{\omega}{v}\right)^2\right],$$

where B is the separation energy of the pair and $\mathcal{A} = (1 + \Delta/\lambda)/2$. Therefore, the cross section is given by

$$\frac{d\sigma}{dq_1\, dq_2} \propto q_1^2 q_2^2 \exp\left[-\frac{\Delta^2}{8\mathcal{A}}\left(q_{1z} + q_{2z} - \frac{\omega}{v}\right)^2\right] \times \exp\left[-\frac{\Delta^2}{8\mathcal{A}}|\mathbf{q}_{1\perp} + \mathbf{q}_{2\perp}|^2\right] \left[\exp\left(-\frac{q_1^2 r_c^2}{4}\right) + \exp\left(-\frac{q_2^2 r_c^2}{4}\right)\right]^2. \tag{29}$$

Now one can easily understand the physics in Fig. 4 by identifying the terms of the above equation. The first term is due to conservation of the momentum along the beam direction, which yields the dispersion relation, Eq. (1). Note that in the derivation of Eq. (19) it was assumed that the core recoils with the same momentum, i.e., $Q_Z \simeq \omega/v = -(q_{1z} + q_{2z})$. The second term is due to elastic scattering of the pair on the target in the direction transverse to the beam. In Eq. (29) both the first and the second terms imply that the momentum distribution of correlated pair is such that $q_1 + q_2 = \omega/v$, i.e., $q_1 \simeq -q_2$, as expected for small r_c. Also according to these terms, the distribution is smeared by the range of the independent wavefunctions of the pair, i.e., $\langle q_{1,2}^2 \rangle \simeq 1/\Delta^2$. However, the last term implies a smearing, or spreading, of the momentum distribution by a much larger factor (assuming $r_c \ll \Delta$), i.e., $\langle q_{1,2}^2 \rangle \simeq 1/r_c^2$. This explains all physics presented in Fig. 4. The second exponential term in Eq. (29) plays no role in the results presented in Fig. 4, since it is identical to one.

As discussed above, the location of the ridges in Fig. 4 is a kinematical property of the phonon absorption mechanism, which is independent of the collision energy. Thus, it should be observable in intermediate energy collisions ($E_{\mathrm{lab}} \simeq 100$ MeV/nucleon), as well as in relativistic collisions. One also observes that the momentum distributions are narrower for correlated-pair emission from a halo nucleus. This is due to the low binding energy, which yields an extended wavefunction of the nucleons in the halo. This is also seen from the first exponential term of Eq. (29), since the two-proton separation energy for ^{12}C is 27.16 MeV, while the two-neutron separation energy in ^{11}Li is 0.3 MeV. The effective value of Δ is much smaller for the first case, leading to a larger spreading of the momentum distributions. However, the last term in Eq. (29) is still the dominant one.

It would be interesting to try to observe the contribution of the emission of correlated pairs in singles spectra. This can be obtained by integrating $d\sigma/dq_1\, dq_2$ over one of the two nucleon momenta. This is shown in Fig. 5 for C + C and Li + Be collisions, using $r_c = 0.7$ fm. One observes that the peak in the singles spectra occurs at $p \simeq \hbar/r_c$, as expected from the arguments presented above. This should be visible in the spectra of nucleons from knockout reactions as a bump at high nucleon momenta. The position of the bump would be a direct reading of the short-range correlation distance. Notice, however, that such a bump might not be noticeable because it is superposed to a large background of knockout nucleons from stripping reactions. Only by doing a measurement of back-to-back pair emission, this signature of short-range pair-correlations could be assessed.

The total cross section for the emission of correlated pairs arising from short-range correlations can be calculated from Eq. (24). Assuming $r_c = 0.7$ fm, the total cross section for the

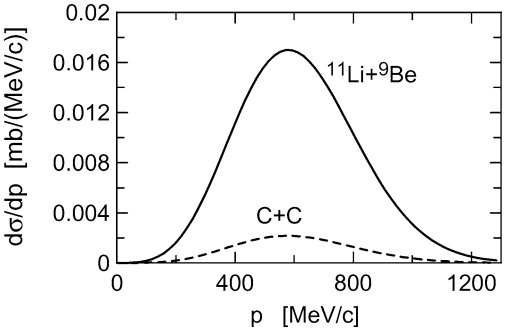

Fig. 5. Singles spectra for the momentum distribution of a nucleon due to the correlated-pair mechanism.

emission of high-energy correlated pairs in C + C collisions at 250 MeV/nucleon is $\sigma_{\rm corr} = 0.61$ mb. The experimental value for two-proton knockout in this collision is 5.88 ± 9.70 mb. For $^{11}\mathrm{Li} + {}^{9}\mathrm{Be}$ at 287 MeV/nucleon the correlated-pair cross section is $\sigma_{\rm corr} = 4.1$ mb. These cross sections are much smaller than those obtained in Refs. [9,10]. For reasons which were explained in the paragraph preceding Eq. (16), the results obtained here are much more reasonable. These cross sections are also much smaller than those for one-nucleon knockout reactions (see, e.g., Ref. [5]). They are also only one of the contributions (i.e., only from diffraction dissociation) of the two-proton removal cross section. Another contribution (stripping) has not been considered here. Stripping would not contribute to back-to-back nucleon emission, with nearly zero total momentum of the pair, but is responsible for the largest part of the two-nucleon knockout total cross section.

In conclusion, I have shown that when a projectile reacts with a light nuclear target, the short-range correlations contribute to the emission of high-energy nucleons which can be visible in measurements of back-to-back emission of nucleon pairs. More experiments and also the development of a more complete reaction theory are interesting challenges. The theoretical results suggest that the pattern and absolute magnitudes of the partial cross sections can provide specific information on the detailed nature of the states involved. This is particularly important in the case of reactions involving neutron-rich and proton-rich nuclei, far from the stability valley, for which only nuclear reactions are presently capable of probing their internal structure. The results presented here will be valuable as a guide to extend these studies towards drip line nuclei and look for effects which cannot be probed in (e, e') scattering due to the lack of experimental facilities for electron scattering on drip line nuclei.

Acknowledgements

I would like to thank Angela Bonaccorso, Kai Hencken and Ian Thompson for beneficial discussions. This work was supported by the US Department of Energy under grant No. DE-FG02-04ER41338.

References

[1] R.J. Glauber, in: W.E. Brittin, L.G. Dunham (Eds.), in: Lectures in Theoretical Physics, vol. 1, Interscience, New York, 1959.
[2] T. Fujita, J. Hüfner, Nucl. Phys. A 343 (1980) 493.
[3] J. Hüfner, M.C. Nemes, Phys. Rev. C 23 (1981) 2538.

[4] C.A. Bertulani, M. Hussein, G. Muenzenberg, Physics of Radioactive Beams, Nova Science, Hauppage, NY, 2002.
[5] P.G. Hansen, J.A. Tostevin, Annu. Rev. Nucl. Part. Sci. 53 (2003) 219.
[6] C.A. Bertulani, G. Baur, Phys. Rep. 163 (1988) 299.
[7] T. Glasmacher, Annu. Rev. Nucl. Part. Sci. 48 (1998) 1.
[8] C.A. Bertulani, V. Ponomarev, Phys. Rep. 321 (1999) 139.
[9] H. Feshbach, M. Zabek, Ann. Phys. 107 (1977) 110.
[10] H. Feshbach, Prog. Part. Nucl. Phys. 4 (1980) 532.
[11] G.E. Brown, P.A. Deutchman, in: Workshop on High Resolution Heavy Ion Physics at $E/A = 20$–100 MeV, 31 May–2 June 1978, Saclay, p. 212.
[12] N.S.P. King, et al., Phys. Lett. B 175 (1986) 279.
[13] L.W. Townsend, P.A. Deutchman, Nucl. Phys. A 355 (1981) 505.
[14] L.W. Townsend, P.A. Deutchman, R.L. Madigan, J.W. Norbury, Nucl. Phys. A 415 (1984) 520.
[15] J.W. Norbury, P.A. Deutchman, L.W. Townsend, Nucl. Phys. A 433 (1985) 691.
[16] P.A. Deutchman, J.W. Norbury, L.W. Townsend, Nucl. Phys. A 454 (1986) 733.
[17] P. Chomaz, N. Frascaria, Phys. Rep. 252 (1995) 275.
[18] L.L. Frankfurt, M.I. Strikman, Phys. Rep. 76 (1981) 215.
[19] L.L. Frankfurt, M.I. Strikman, Phys. Rep. 160 (1988) 235.
[20] S.S. Dimitrova, et al., Eur. Phys. J. A 7 (2000) 335.
[21] C. Barbieri, W.H. Dickhoff, Phys. Rev. C 65 (2002) 064313.
[22] A. Tang, et al., Phys. Rev. Lett. 90 (2003) 042301.
[23] J. Ryckebusch, W. van Nespen, Eur. Phys. J. A 20 (2004) 435.
[24] V.R. Pandharipande, et al., Rev. Mod. Phys. 69 (1997) 981.
[25] C.A. Bertulani, L.F. Canto, R. Donangelo, J.O. Rasmussen, Mod. Phys. Lett. A 4 (1989) 1315.
[26] F.S. Navarra, M.C. Nemes, Phys. Rev. C 43 (1991) R939.
[27] D. Bazin, B.A. Brown, C.M. Campbell, J.A. Church, D.C. Dinca, J. Enders, A. Gade, T. Glasmacher, P.G. Hansen, W.F. Mueller, H. Olliver, B.C. Perry, B.M. Sherrill, J.R. Terry, J.A. Tostevin, Phys. Rev. Lett. 91 (2002) 012501.
[28] C.A. Bertulani, P. Danielewicz, Introduction to Nuclear Reactions, IOP Publishing, London, 2004, p. 419.
[29] K. Hencken, H. Esbensen, G. Bertsch, Phys. Rev. C 54 (1996) 3043.
[30] M.H. MacGregor, A.R. Arndt, R.M. Wright, Phys. Rev. 182 (1969) 1714.
[31] A. Bohr, B. Mottelson, Nuclear Structure, vol. 1, Benjamin, New York, 1969.
[32] R. Jastrow, Phys. Rev. 98 (1955) 1479.
[33] L.C. Gomes, J.D. Walecka, V.F. Weisskopf, Ann. Phys. (N.Y.) 3 (1958) 241.
[34] L. Ray, Phys. Rev. C 20 (1979) 1859.
[35] E. Boridy, H. Feshbach, Ann. Phys. (N.Y.) 109 (1977) 468.
[36] M.S. Hussein, R. Rego, C.A. Bertulani, Phys. Rep. 201 (1991) 279.
[37] J.A. Tostevin, G. Podolyák, B.A. Brown, P.G. Hansen, Phys. Rev. C 70 (2004) 064602.
[38] H. Simon, D. Aleksandrov, T. Aumann, L. Axelsson, T. Baumann, M.J.G. Borge, L.V. Chulkov, R. Collatz, J. Cub, W. Dostal, B. Eberlein, Th.W. Elze, H. Emling, H. Geissel, A. Gruenschloss, M. Hellstrom, J. Holeczek, R. Holzmann, B. Jonson, J.V. Kratz, G. Kraus, R. Kulessa, Y. Leifels, A. Leistenschneider, T. Leth, I. Mukha, G. Muenzenberg, F. Nickel, T. Nilsson, G. Nyman, B. Petersen, M. Pfützner, A. Richter, K. Riisager, C. Scheidenberger, G. Schrieder, W. Schwab, M.H. Smedberg, J. Stroth, A. Surowiec, O. Tengblad, M.V. Zhukov, Phys. Rev. Lett. 83 (1999) 496.
[39] C.A. Bertulani, P.G. Hansen, Phys. Rev. C 70 (2004) 034609.
[40] P.G. Hansen, Nucl. Phys. A 682 (2001) 310.